

**Outflows from accreting super-spinars**Cosimo Bambi,<sup>1,\*</sup> Tomohiro Harada,<sup>2,†</sup> Rohta Takahashi,<sup>3,‡</sup> and Naoki Yoshida<sup>1,§</sup><sup>1</sup>*Institute for the Physics and Mathematics of the Universe, The University of Tokyo, Kashiwa, Chiba 277-8583, Japan*<sup>2</sup>*Department of Physics, Rikkyo University, Toshima, Tokyo 171-8501, Japan*<sup>3</sup>*Cosmic Radiation Laboratory, The Institute of Physical and Chemical Research, Wako, Saitama 351-0198, Japan*

(Received 31 March 2010; published 4 May 2010)

In this paper we continue our study on the accretion process onto superspinning Kerr objects with no event horizon (super-spinars). We discuss the counterpart of the Bondi accretion onto black holes. We first report the results of our numerical simulations. We found a quasi-steady-state configuration for any choice of the parameters of our model. The most interesting feature is the presence of hot outflows. Unlike jets and outflows produced around black holes, which are thought to be powered by magnetic fields and emitted from the poles, here the outflows are produced by the repulsive gravitational force at a small distance from the super-spinar and are ejected around the equatorial plane. In some circumstances, the amount of matter in the outflow is considerable, which can indeed significantly reduce the gas mass accretion rate. Finally, we discuss a possible scenario of the accretion process in more realistic situations, which cannot be simulated by our code.

DOI: 10.1103/PhysRevD.81.104004

PACS numbers: 04.20.Dw, 95.30.Lz, 97.10.Gz, 97.60.-s

**I. INTRODUCTION**

The actual nature of the final product of the gravitational collapse of matter is an outstanding and long-standing problem in general relativity (GR). Under apparently reasonable assumptions, collapsing matter leads to the formation of space-time singularities [1]. Here there are two possibilities: (i) the singularity is hidden behind an event horizon and the final product is a black hole (BH), or (ii) the singularity is naked. Since space-times with naked singularities present pathologies, some form of the cosmic censorship conjecture is usually assumed and naked singularities are forbidden [2]. Neglecting the electric charge, it turns out that, in four dimensions, the only stationary and asymptotically flat solution of the vacuum Einstein equation with an event horizon is the Kerr BH [3,4].

The Kerr metric is completely characterized by two parameters; that is, the mass  $M$  and the spin  $J$ . The latter is often replaced by the Kerr parameter  $a$ , defined as  $a = J/M$ , or by the dimensionless Kerr parameter  $a_* = a/M$ . Using Boyer-Lindquist coordinates, the position of the horizon of a Kerr BH is given by

$$r_H = M(1 + \sqrt{1 - a_*^2}), \quad (1)$$

which demands the well known constraint  $|a_*| \leq 1$ . For  $|a_*| > 1$ , there is no horizon and the space-time has a naked singularity. Since causality can be violated in Kerr space-times with no event horizon [5,6], the assumption of the cosmic censorship conjecture appears well motivated.

Interestingly, several solutions of the Einstein equations that lead to the formation of naked singularities are known (see e.g. Refs. [7–12]). Moreover, the reliability of GR at the singularity is surely questionable. GR is a classical theory and it is widely believed that the Planck scale,  $E_{\text{Pl}} \sim 10^{19}$  GeV, is its natural UV cutoff. New physics needs to replace the singularity with something else [13]; then the space-time in the full theory may present no pathologies. If this is the case, the cosmic censorship conjecture may not be necessary and superspinning Kerr objects with no event horizon, or “super-spinars,” may exist in the Universe [14].

A subtle point is the stability of these objects, but the issue is not so easy to address, especially because we do not know the actual space-time emerging from the full theory. The simplest kind of instability is represented by the process of accretion itself, which may reduce  $|a_*|$  and convert the super-spinar into a BH [15]. However, the evolution of the Kerr parameter due to accretion is usually negligible in stellar mass objects in binary systems and, as discussed in this paper, the accretion onto super-spinars is strongly suppressed, because of the presence of powerful outflows. A different issue is the intrinsic stability of the space-time. A “true” Kerr naked singularity is *probably* unstable [16,17], but such a conclusion is based on an analysis of the whole Kerr space-time with  $-\infty < r < +\infty$ , which includes “another Universe,” connected to “our Universe” through the singularity and admitting closed timelike curves. Another danger is represented by the so-called ergo-region instability [18,19]. The stability of the space-time is, however, mainly determined by the boundary conditions, which are unknown in our case. The motivation to consider super-spinars is that high-energy corrections to classical GR may replace the singularity with something else and that the space-time has no path-

\*cosimo.bambi@ipmu.jp

†harada@rikkyo.ac.jp

‡rohta@riken.jp

§naoki.yoshida@ipmu.jp

ologies in the full theory. Since we do not know the full theory, we cannot predict the actual structure of the space-time at very small radii. Here we do not further discuss this point: we simply assume that super-spinars are stable or quasistable objects. We study their astrophysical implications. Let us also notice that, even if super-spinars were unstable, they may still be a possible intermediate state of the gravitational collapse, before decaying into spinning BHs after some characteristic time scale. Their astrophysical implications may still be very intriguing.

It is thus interesting to look for observational signatures capable of distinguishing super-spinars from ordinary BHs, with present and future astrophysical experiments. References [20,21] discussed the implications on the apparent shape. There it was found that, even if the bound  $|a_*| \leq 1$  is violated by a small amount, the shadow cast by the super-spinar (i.e. how it blocks light coming to us from an object behind it) changes significantly from the BH case: the shadow for the super-spinar is about an order of magnitude smaller as well as distorted. This distinction can be used as an observational signature in the search for these objects. Based on recent observations at mm wavelength of the supermassive BH candidate at the center of the Galaxy [22], in [20] one of us speculated on the possibility that it might violate the Kerr bound.

The x-ray thermal spectrum emitted by an optically thick and geometrically thin accretion disk around a super-spinar was instead investigated in [23]. Surprisingly, for any BH with Kerr parameter  $a_*^{\text{BH}}$ , there is a super-spinar with Kerr parameter  $a_*^{\text{SS}}$  in the range  $[5/3; 8\sqrt{6}/3]$  whose spectrum is very similar (and practically indistinguishable) from the one of the BH. The result is that the x-ray thermal spectrum observed from current BH candidates cannot be used to confirm the Kerr bound  $|a_*| \leq 1$ . However, the contrary is *not* true: the x-ray thermal spectrum of a super-spinar with  $1 < |a_*| < 5/3$  can be significantly different from the one of BH. The disk temperature is higher and the radiation flux larger, even by a few orders of magnitude for  $|a_*|$  slightly larger than 1. In principle, this could be used to distinguish super-spinars from BHs.

In this paper, we extend the study on the accretion process onto super-spinars started in [24]. Here we consider the counterpart of the Bondi accretion onto BHs. In the case of BHs, this is a quite inefficient mechanism to convert the gravitational energy into radiation, because a large fraction of the thermal energy is lost behind the horizon. The efficiency is  $\eta \sim 10^{-4}$  and thus the Bondi accretion cannot explain many of the observed BH candidates. In the case of super-spinars, the efficiency can be much higher. As shown in [24], near super-spinars there are space regions where the gravitational force is repulsive. In the Bondi-like case, the gas approaches the compact object with high velocity, enters the region with repulsive gravitational force, and slows down. Some amount of gas, which

depends on the spin and the actual size of the super-spinar, is eventually ejected away, preferably on the equatorial plane. Unlike the case of an accretion flow of low temperature and low velocity discussed in [24], here the gas reaches the center preferably from the axis of symmetry (rather than from the equatorial plane) and we find the production of hot outflows, which can have quite interesting implications. Since outflows produced in the accretion process onto BHs are expected to be emitted from their poles, the possible observation of powerful equatorial outflows from a BH candidate could be evidence that such an astrophysical object is actually a super-spinar or, more in general, a spinning supercompact object with no event horizon.

The paper is organized as follows. In Sec. II, we briefly summarize the results obtained in [24]. In Sec. III, we present the results of our simulations of the Bondi-like accretion onto super-spinars. In Sec. IV, we discuss the role of the free parameters of our model and how their variation changes the accretion process. On the basis of such numerical study, in Sec. V we discuss a possible scenario in more realistic cases, mentioning physical and astrophysical implications. Summary and conclusions are reported in Sec. VI. Throughout the paper we use Boyer-Lindquist coordinates to describe the Kerr background and natural units  $G_N = c = k_B = 1$ .

## II. SUMMARY OF THE PREVIOUS WORK

In this section, we briefly review the basic results found in [24] (see also the discussion in [25]). There, we studied the accretion process of a test fluid in a background Kerr space-time; that is, we neglected the backreaction of the fluid to the geometry of the space-time, as well as the growth in mass and the variation in spin of the central object due to accretion. Such an approximation can be used if we want to study, for instance, the accretion of a stellar mass compact object in a binary system, because in this case the matter captured from the stellar companion is typically small in comparison with the total mass of the compact object. On the other hand, it is not appropriate to study long-term accretion onto a supermassive object at the center of a galaxy, where accretion makes the mass of the compact object increase by a few orders of magnitude from its original value.

The calculations were made with the relativistic hydrodynamics module of the public available code PLUTO [26,27], properly modified for the case of curved space-time [28]. As equation of state of the accreting matter, we used the one of an ideal gas with polytropic index  $\Gamma = 5/3$ . We adopted Boyer-Lindquist coordinates to describe the Kerr background. The computational domain was the 2D axisymmetric space  $r_{\text{in}} < r < 20M$  and  $0 < \theta < \pi$ , where  $r_{\text{in}}$  was set just outside the event horizon in the case of BH, and  $r_{\text{in}} = 0.5M$  in the case of super-spinar. The choice of  $r_{\text{in}} = 0.5M$  may appear arbitrary, but it was checked that it

does not significantly alter the final result for any value of  $a_*$ , as long as  $r_{\text{in}} \lesssim 0.7M$ .

We injected gas from the outer boundary into the computational domain isotropically at a constant rate, with low velocity (specifically,  $v^r = -0.0001$  and  $v^\theta = v^\phi = 0$ ). Because of the simple treatment of the accreting matter, the gas temperature was not under control. In [24], we simply imposed a maximum temperature: the aim was not to find an accurate description of the process, but only to capture some characteristic features of the accretion in Kerr space-times with  $|a_*| > 1$ . The code was run with  $T_{\text{max}} = 10$  keV, 100 keV, and 1 MeV, yielding essentially the same result. Such a range of  $T_{\text{max}}$  is the one suggested by observations of galactic BH candidates: the hard x-ray continuum (10–200 keV) is a typical feature of all these objects and is often explained with a hot inner disk or a hot corona, in which the electron temperature is around 100 keV (see e.g. Ref. [29]). Let us notice that this is not the Bondi accretion. The temperature of the gas (ions) at the horizon (in the case of BHs) in the Bondi accretion is about 100 MeV.

In [24], we found that the accretion process for  $|a_*| > 1$  is strongly influenced by the existence of regions near the massive object in which the gravitational force is repulsive. Such a repulsive force is not an inertial effect due to the rotation of the gas, but arises from the presence of the naked singularity and is probably a quite common feature in space-times with naked singularities. In particular, for super-spinars with  $|a_*| < 1.4$ , the accretion process is extremely suppressed and only a small amount of the accreting gas can reach the center. Most of the gas is accumulated around the object, forming a high density cloud that continues to grow. No quasi-steady state was found.

### III. BONDI-LIKE ACCRETION ONTO SUPER-SPINARS

The “standard” Bondi accretion describes a spherical, steady-state, and adiabatic accretion onto an object. Spherical or quasispherical accretion flows are expected when the compact object accretes from the interstellar medium or when it belongs to a binary system in which the companion is massive and has a strong stellar wind. The basic features of the Bondi accretion onto a Schwarzschild BH can be deduced analytically [30] (see also Appendix G of Ref. [31]). The proper velocity of the fluid at the horizon as measured by a local stationary observer is equal to 1. For  $\Gamma = 5/3$ , the fluid temperature at the horizon is independent of the temperature at infinity and is given by

$$T_H \approx \frac{3}{40} \left( \frac{2}{u_H^2} \right)^{1/3} m \approx 105 \left( \frac{m}{940 \text{ MeV}} \right) \text{ MeV}, \quad (2)$$

where  $u_H$  is the inward radial component of the 4-velocity at the horizon ( $u_H \approx 0.782$  for  $\Gamma = 5/3$ ) and  $m$  is the mean baryon mass. The accretion luminosity is low, because

most of the thermal energy is advected into the horizon and lost. The efficiency parameter is  $\eta \sim 10^{-4}$ , which is much lower than the usual value 0.1–0.3 estimated from observations.

The counterpart of the Bondi accretion in the case of super-spinar presents some peculiar features. The accretion process near the object is clearly far from being spherically symmetric, as the space-time geometry is only axially symmetric. Moreover, even the adiabatic description does not work at very small radii, because some amount of fluid is heated to very high temperatures. Despite that, far from the compact object the conditions are the same of the usual Bondi accretion.

With a slightly improved version of the code used in [24], we have studied numerically the Bondi-like accretion process onto super-spinars. The setup is almost the same as in Ref. [24]. The default size of the computational domain is still the 2D axisymmetric space  $r_{\text{in}} < r < r_{\text{out}}$  and  $0 < \theta < \pi$ , with  $r_{\text{in}} = 0.5M$  and  $r_{\text{out}} = 20M$ . The initial and boundary conditions are similar, except for the radial velocity with which the gas is injected from the computational domain. In the Bondi accretion, the fluid is almost in free fall, and we thus take

$$v^r \approx -\sqrt{\frac{M}{r_{\text{out}}}} \approx -0.224, \quad (3)$$

instead of the very small value adopted in the previous work. As in [24], the boundary conditions at  $r_{\text{in}}$  are such that the boundary behaves as a perfectly absorbing surface: the gas in the computational domain can flow to the outside, but no gas can enter the computational domain from the boundary.

The most important ingredient in the new simulations is that now the temperature of the gas is everywhere under control, except in a small region at the inner boundary where the repulsive gravitational force is stronger. Here the gas temperature becomes too high.<sup>1</sup> In the Bondi accretion onto a Schwarzschild BH, for a fluid with  $\Gamma = 5/3$ , the temperature scales as  $1/r$  because the gravitational energy is efficiently converted to thermal energy. The temperature at the horizon is about 100 MeV. In this paper we imposed  $T_{\text{max}} = 1$  GeV as our “canonical” value. For example, the energy of a free particle in the Kerr space-time is

<sup>1</sup>The reason is probably that PLUTO works with weak force fields, but finds difficulties otherwise. For example, even the public version of the code shows a similar behavior in the case of accretion onto a pointlike mass in Newtonian gravity, when one includes the region close to the object (where actually Newtonian gravity should not be used). The same problem exists in our simulations of the accretion onto an ordinary BH, if the inner boundary is close to the horizon. Nevertheless, since the gravitational force around a BH is always attractive, in the latter case the hot gas does not escape: so we do not have under control its temperature in such a region, but there are no effects on the accreting gas at larger distances.

$$E = \left(1 - \frac{2Mr}{r^2 + a^2 \cos^2 \theta}\right) u^t + \frac{2aMr \sin^2 \theta}{r^2 + a^2 \cos^2 \theta} u^\phi, \quad (4)$$

where  $u^t$  and  $u^\phi$  are, respectively, the  $t$  and  $\phi$  components of the particle 4-velocity. If the gravitational energy were efficiently converted to thermal energy, on the equatorial plane the gas temperature would still roughly scale as  $1/r$  and would diverge at the singularity. For  $r = 0.5M$ , we would find  $T \sim 0.5$  GeV. However, around a super-spinar the gas can be further heated by the collisions between the inflowing and outflowing matter. Thus we set  $T_{\max} = 1$  GeV. We also study the dependence of the accretion process on  $T_{\max}$  in Sec. IV A. We show that the choice of  $T_{\max}$  does not significantly affect the overall behavior of the flow around super-spinars.

Let us notice that here we use the same description for the gas in the whole computational domain. At very high temperatures, the degrees of freedom, as well as the gas equation of state, change. Nevertheless we treat the accreting matter as an ideal gas. Namely, we assume that the correct qualitative picture of the accretion process can be described even neglecting such effects. Actually, these uncertainties should be considered together with the inner boundary conditions. In our simulations, we take  $r_{\text{in}} = 0.5M$ , but the actual size of the massive objects could be much smaller. At very small distances from the center, the density and the temperature of the gas can become extremely high, and our physics should not be used. In Sec. V, we extrapolate from our numerical study a possible picture that appears physically reasonable.

The Bondi-like accretion onto super-spinars presents some very interesting features that were absent in our previous study. In Ref. [24], the velocity of the gas was low and only a very small fraction of it was able to enter the region with repulsive gravitational force. Such a region was indeed almost empty. Now instead the fluid approaches the massive object with a much higher velocity,

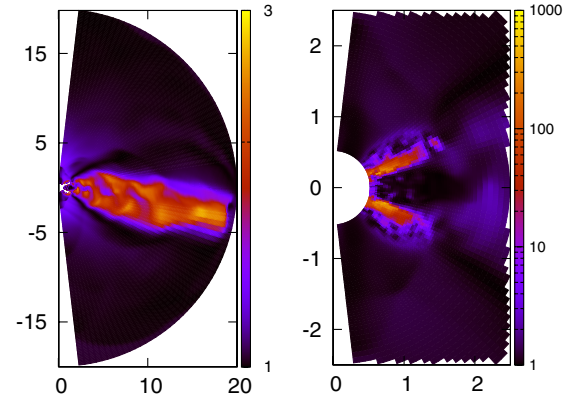


FIG. 2 (color online). Snapshot at  $t = 1000M$  of the Lorentz factor  $\gamma = 1/\sqrt{1 - v^2}$  of the accreting gas around a super-spinar with  $a_* = 1.5$ , for  $T_{\max} = 1$  GeV. The unit of length along the  $x$  and  $y$  axes is  $M$ .

and it thus can enter the region where the net gravitational force is repulsive. Because of the pressure of the fluid, the gas is compressed where the repulsive gravitational force is strong. The gas is then heated and eventually ejected to larger radii. The amount of gas ejected and its energy do depend on the spin of the compact object, i.e.  $a_*$ , and the temperature of the gas ejected (in our case  $T_{\max}$ ), as discussed in the next section.

Density, temperature, and radial velocity of the gas as computed by our code are shown in Fig. 1 for the case  $a_* = 1.5$ , with  $T_{\max} = 1$  GeV. In Fig. 2, we show the Lorentz factor  $\gamma = 1/\sqrt{1 - v^2}$  and, in Fig. 3, the direction of the velocity of the accreting gas in the plane  $(r, \theta)$ . Figure 1 can be compared with Fig. 4, where we show the same quantities as computed by our code for a Kerr BH with  $a_* = 0.99$  and  $r_{\text{in}} = 2.5M$  (no  $T_{\max}$  is necessary here). Since we are discussing the Bondi accretion without the presence of magnetic fields, in the BH case there are no outflows.

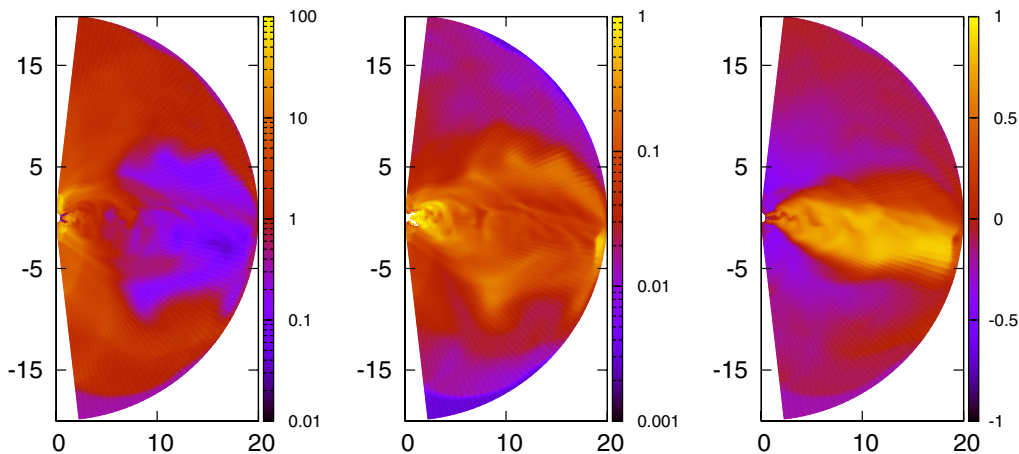


FIG. 1 (color online). Snapshot at  $t = 1000M$  of the density  $\rho$  (left panels: density in arbitrary units), temperature  $T$  (central panel: temperature in GeV), and contravariant radial component of the 3-velocity  $v^r$  (right panels: velocity in unit  $c = 1$ ) of the accreting gas around a super-spinar with  $a_* = 1.5$ , for  $T_{\max} = 1$  GeV. The unit of length along the  $x$  and  $y$  axes is  $M$ .

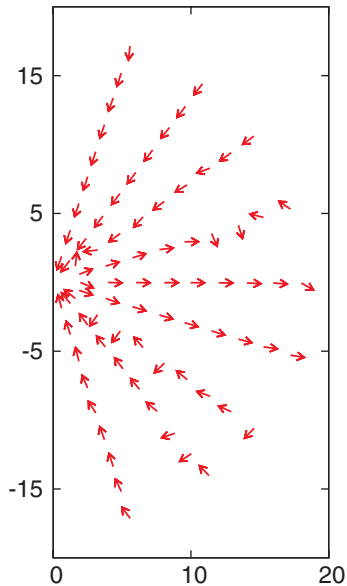


FIG. 3 (color online). Snapshot at  $t = 1000M$  of the direction of the velocity of the accreting gas around a super-spinar with  $a_* = 1.5$ , for  $T_{\max} = 1$  GeV. The unit of length along the  $x$  and  $y$  axes is  $M$ .

#### IV. DEPENDENCE ON $T_{\max}$ , $r_{\text{in}}$ , AND $a_*$

The setup of our simulations is basically characterized by three free parameters: the maximum temperature  $T_{\max}$ , the inner radius of the computational domain  $r_{\text{in}}$ , and the dimensionless Kerr parameter  $a_*$ . In order to elucidate their effects on the accretion process, we introduce two physical quantities: the mass accretion rate of the space inside the radius  $r = 5M$ , that is,

$$\dot{M}_{\text{acc}}(t) = \int_{r=5M} \rho v^r \sqrt{\gamma} d\theta d\phi, \quad (5)$$

and its time integral, i.e. the accreted mass of the space

inside the radius  $r = 5M$ :

$$M_{\text{acc}}(t) = \int_{t_0}^t \dot{M}_{\text{acc}}(\tau) d\tau. \quad (6)$$

The temporal behavior of  $\dot{M}_{\text{acc}}$  and  $M_{\text{acc}}$  in the interval  $0 < t < 1000M$  are presented in Fig. 5 for our default choice  $a_* = 1.5$  and  $T_{\max} = 1$  GeV, and can be compared with the ones for a BH with  $a_* = 0.99$ , presented in Fig. 6. In the latter case, for  $t \geq 150M$ ,  $\dot{M}_{\text{acc}}$  is exactly the amount of mass injected from the boundary (in our simulations 425, in arbitrary units).

#### A. Maximum temperature of the gas

Our simulations require the imposition of a maximum temperature in order to avoid unphysical results. We thus need to set  $T_{\max}$ . It should depend on physical processes that are neglected in our code (e.g. cooling mechanisms), on the choice of  $r_{\text{in}}$ , and even on the phenomena occurring at smaller radii (where actually we cannot predict reliably what happens). It is natural to expect that a lower (higher) value of  $T_{\max}$  leads to less (more) energetic outflows and thus the accretion rate is less (more) suppressed. This is indeed confirmed by the simulations: in Fig. 7, we show the mass accretion rate and the accreted mass for  $T_{\max} = 500$  MeV (top panels) and 2 GeV (bottom panels), still for  $a_* = 1.5$ . A maximum temperature of 2 GeV at  $r = 0.5M$  is likely too high, but it is useful to figure out the effect of  $T_{\max}$  on the accretion process and check the response of our code. At the beginning,  $0 < t < 200M$ , the accretion process strongly depends on the initial conditions, but seems also to give a rough idea of the mass accretion rate at later time. As  $T_{\max}$  increases, the accreted mass at  $t = 200M$  decreases. As shown in the next two subsections, the idea that the accreted mass at  $t = 200M$  can suggest how much the accretion process is suppressed at later time seems to be correct even for the other two free

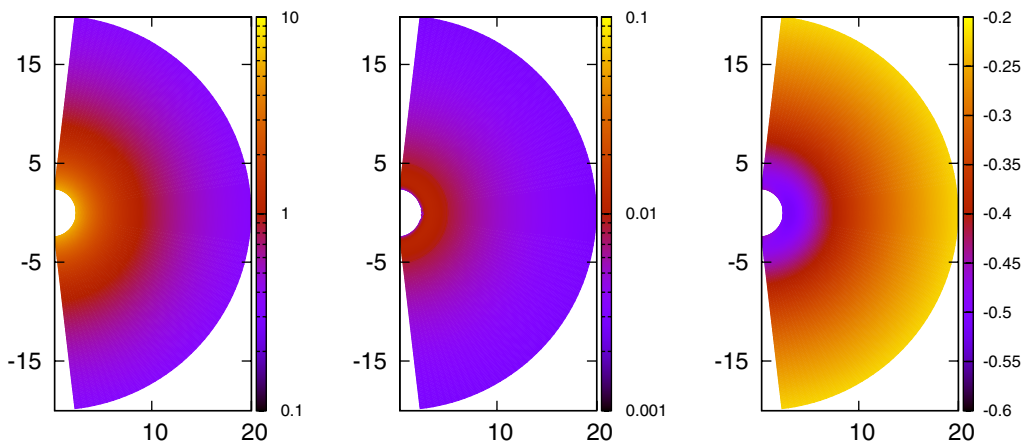


FIG. 4 (color online). Density  $\rho$  (left panels: density in arbitrary units), temperature  $T$  (central panel: temperature in GeV), and contravariant radial component of the 3-velocity  $v^r$  (right panels: velocity in unit  $c = 1$ ) of the quasiequilibrium configuration of the accreting gas around a Kerr black hole with  $a_* = 0.99$ . The unit of length along the  $x$  and  $y$  axes is  $M$ .

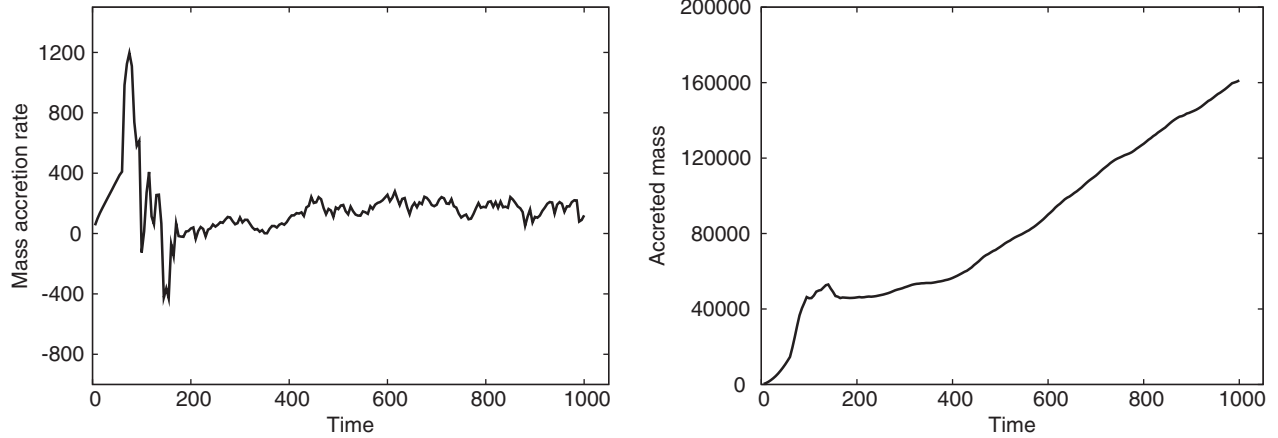


FIG. 5. Mass accretion rate (left panel) and accreted mass (right panel) as a function of time  $t$  of the space region inside the radius  $r = 5M$  in the case  $a_* = 1.5$  and  $T_{\max} = 1$  GeV.  $\dot{M}_{acc}$  and  $M_{acc}$  in arbitrary units;  $t$  in unit  $M = 1$ .

parameters, i.e.  $r_{in}$  and  $a_*$ . For  $t > 200M$ , the accretion process is more regular and the system reaches quasiequilibrium configurations. In some cases, we observe counter-intuitive results: for example, for  $t > 400M$ , the mass accretion rate for  $T_{\max} = 500$  MeV is lower than the one with  $T_{\max} = 1$  GeV (the slope of the curve of the accreted mass is less steep). This is because the system has not yet reached a quasi-steady state at  $t = 1000M$ . We checked this point by rerunning the code for these two specific cases for a longer time. As shown in Fig. 8, at later time the accretion process is less suppressed for the case with lower temperature, even if the result is not so sensitive to whether we choose  $T_{\max} = 1$  GeV or  $T_{\max} = 500$  MeV. That is good news, because it means that the choice of  $T_{\max}$  is not so important.

### B. Radius of the inner boundary

As the singularity is approached, some observer independent quantities (e.g. the Kretschmann scalar  $K =$

$R_{\kappa\lambda\mu\nu}R^{\kappa\lambda\mu\nu}$ ) diverge. It is usually interpreted as the breakdown of classical GR. Corrections from new physics become presumably more and more important, and it is likely that in the full theory there is no central singularity. If deviations from the classical Kerr metric are negligible as long as these scalars are much smaller than 1 (in Planck units), the simulations should run with  $r_{in}$  as small as possible. Indeed, according to this criterion, for astrophysical objects with mass  $M$  much larger than the Planck mass,  $M_{Pl} \approx 10^{-5}$  g, the classical metric should be reliable up to very small distances from the center, i.e. for  $r \ll M$ . However, it is impossible in practice to run the code with  $r \ll M$ : as  $r_{in}$  decreases, the computational time increases very quickly. In practice, we cannot integrate the system long enough for  $r_{in} < 0.3M$ . In order to catch the effects of a variation of the value of  $r_{in}$  on the accretion process, we studied what happens if we change the value of  $r_{in}$ . Specifically, we run the code with  $r_{in} = 0.3M, 0.8M, 1.0M, 1.2M, 1.5M, 1.6M$ , and  $1.7M$ , for  $T_{\max} = 1$  and  $2$  GeV.

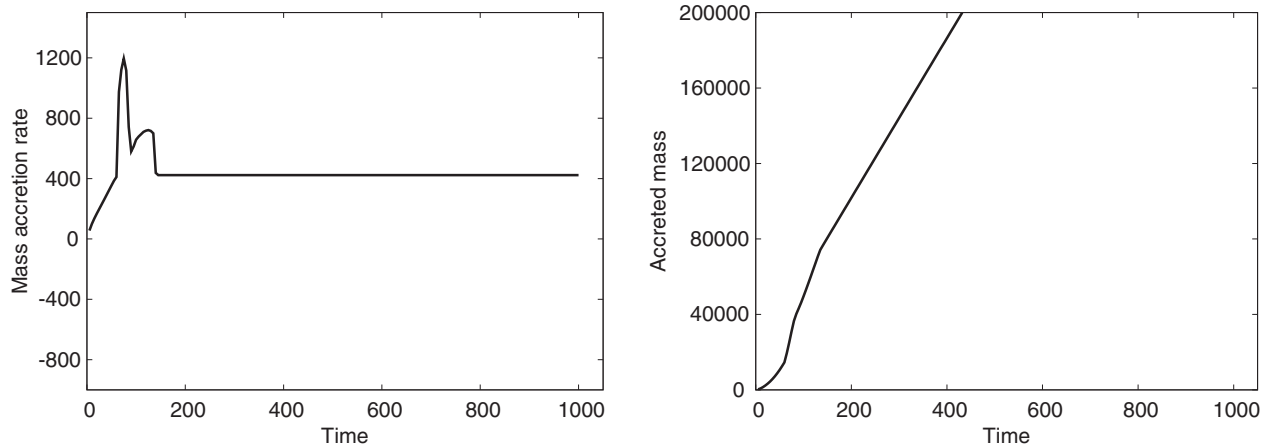


FIG. 6. Mass accretion rate (left panel) and accreted mass (right panel) as a function of time  $t$  of the space region inside the radius  $r = 5M$  in the case of black hole with  $a_* = 0.99$ . For  $t \geq 150$ , the mass accretion rate is exactly the amount of mass injected from the boundary.  $\dot{M}_{acc}$  and  $M_{acc}$  in arbitrary units;  $t$  in unit  $M = 1$ .

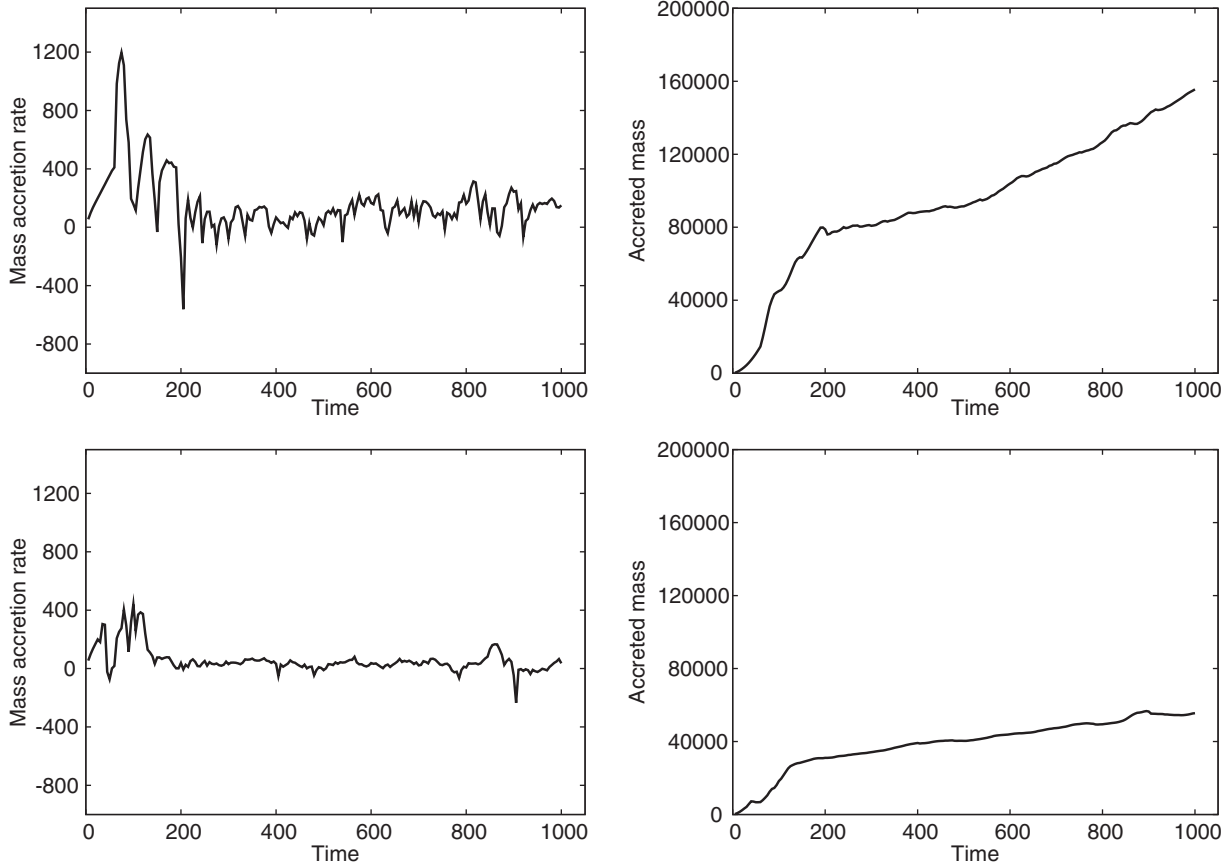


FIG. 7. Mass accretion rate (left panels) and accreted mass (right panels) at  $r = 5M$  for a Kerr super-spinner with  $a_* = 1.5$  for  $T_{\max} = 500$  MeV (top panels) and  $T_{\max} = 2$  GeV (bottom panels).  $\dot{M}_{acc}$  and  $M_{acc}$  in arbitrary units;  $t$  in unit  $M = 1$ .

Roughly speaking, for smaller/larger values of  $r_{in}$ , the accretion rate is lower/higher. This is indeed naively expected: at smaller radii, the density and the pressure of the gas are inevitably higher, reducing the flow velocity. Moreover, the gravitational force close to the center is mainly repulsive, which makes it more and more difficult to push the gas into smaller and smaller radii. However, a more detailed study shows the following features.<sup>2</sup> For  $0.3M \lesssim r_{in} \lesssim 1.2M$ , there is no significant difference in the accretion process (adopting the same value for  $T_{\max}$ , while for smaller  $r_{in}$  one could assume higher maximum temperatures). For  $1.2M \lesssim r_{in} \lesssim 1.6M$ , a slightly higher value of  $r_{in}$  makes the accretion rate much faster and, for  $r_{in} \gtrsim 1.7M$ , the space region with repulsive gravitational force is outside the computational domain and the accretion process is like the one of BH.

### C. Kerr parameter

In Ref. [24], we discussed an accretion process characterized by a gas with low velocity and low temperature.

<sup>2</sup>Here we describe the case  $a_* = 1.5$ . Since the spin parameter determines the region with repulsive gravitational force, for another choice of  $a_*$  one finds a different dependence on  $r_{in}$ .

There we found that, for small  $|a_*|$ , the accretion is extremely suppressed: the gas cannot reach the central massive object, but is instead accumulated around it, forming a high density cloud that continues to grow. As  $|a_*|$  increases, a larger amount of gas can fall to the center and, for  $|a_*| \geq 1.4$ , a quasi-steady-state configuration exists. In the Bondi-like accretion, the picture is very different, and, for higher  $|a_*|$ , the mass accretion rate decreases. That can be explained by noting that, for higher  $|a_*|$ , the repulsive gravitational force close to the center becomes stronger, thus producing more powerful outflows of gas. In Ref. [24], the gas was essentially unable to go to the region where gravity is repulsive, and so we observed neither outflows nor this dependence on the Kerr parameter.

In Fig. 9, we show the mass accretion rate and the accreted mass assuming  $T_{\max} = 1$  GeV and  $r_{in} = 0.5M$ . For  $a_* = 1.1$  and  $1.2$ , the accretion process at  $r = 5M$  is similar to the one onto BH of Fig. 6. Actually there are continuous puffs of hot gas, but their energy is so small that this gas is pushed back by the accreting fluid. Specifically, for  $a_* = 1.1$  the convective region has a radius  $r \approx M$ , while for  $a_* = 1.2$  we find  $r \approx 3M$ ; see Fig. 10. There is no gas that leaves the computational domain from the outer boundary, exactly like in the BH case. For  $|a_*| \geq 1.3$ , the

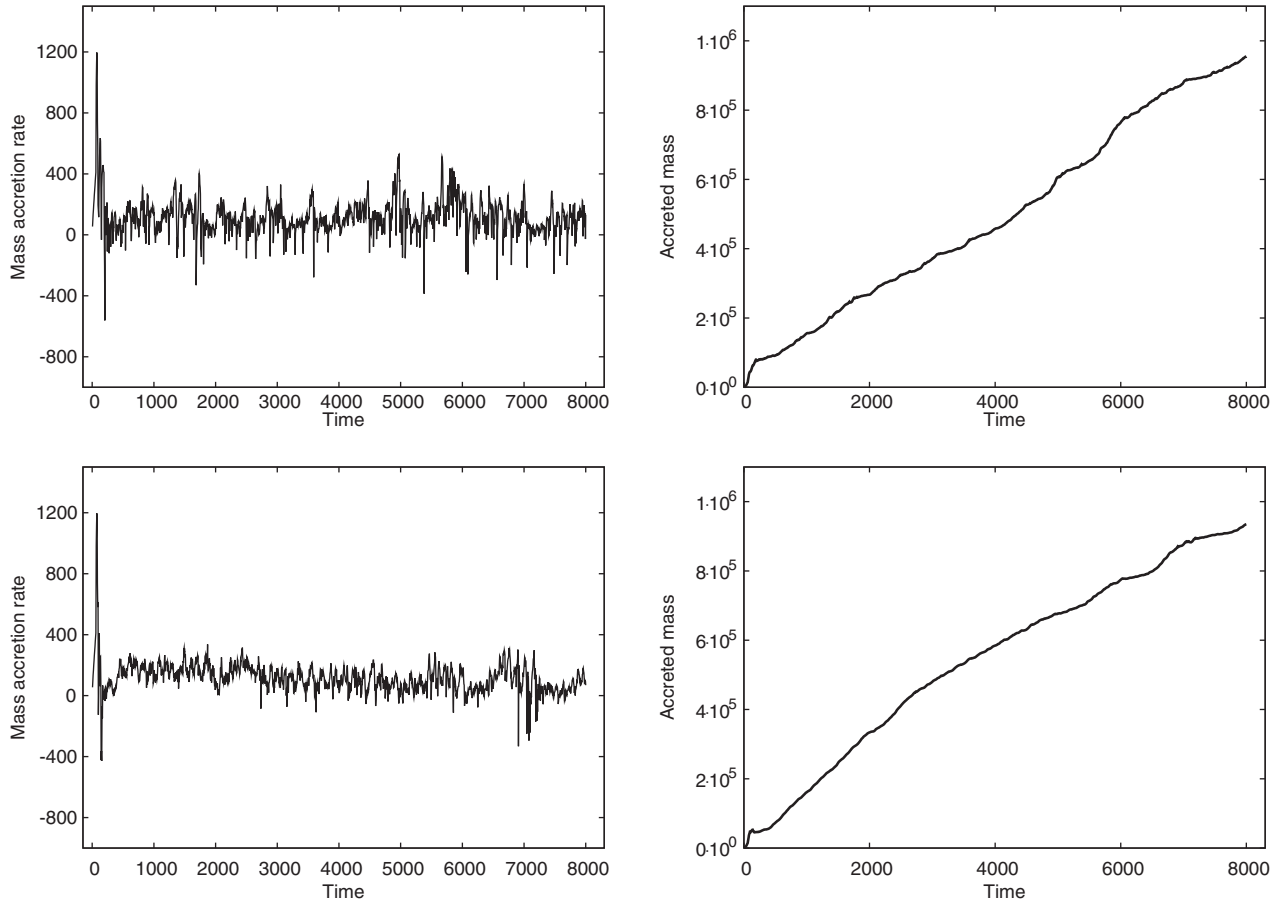


FIG. 8. Mass accretion rate (left panels) and accreted mass (right panels) at  $r = 5M$  for a Kerr super-spinner with  $a_* = 1.5$  for  $T_{\max} = 500$  MeV (top panels) and  $T_{\max} = 1$  GeV (bottom panels) up to  $t = 8000M$ .  $\dot{M}_{acc}$  and  $M_{acc}$  in arbitrary units;  $t$  in unit  $M = 1$ .

outflows are strong enough to leave the region around the center and eventually go out of the computational domain at  $r = r_{\text{out}}$ . We checked that the critical value of the Kerr parameter separating the two different cases is essentially independent of  $r_{\text{in}}$  (for fixed  $T_{\max}$ ), while it is sensitive to the value of  $T_{\max}$ ; i.e. for higher maximum temperature the critical value of the Kerr parameter is a bit smaller. However, it presumably depends on  $r_{\text{out}}$  and the actual size of the accreting cloud around the super-spinner. For an infinite size accreting cloud, we should probably always find a convective region, whose radius increases for higher values of  $|a_*|$  (and  $T_{\max}$ ).

To understand qualitatively the effect of  $a_*$  on the accretion process, we consider the radial component of the geodesic equation of a test particle. To get a rough estimate, we can assume  $\dot{\theta} = 0$  and thus

$$\ddot{r} = -\Gamma_{tt}^r \dot{t}^2 - 2\Gamma_{t\phi}^r \dot{t} \dot{\phi} - \Gamma_{rr}^r \dot{r}^2 - \Gamma_{\phi\phi}^r \dot{\phi}^2, \quad (7)$$

since all the other terms vanish.  $\ddot{r}$  depends on three constants of motion; that is, the particle energy at infinity  $E$ , the  $z$  component of the angular momentum at infinity  $L_z$

(where  $z$  is the axis parallel to the spin of the massive object), and the Carter constant  $Q$ . Let us take  $E = m$  (marginally bound orbit;  $m$  is the mass of the test particle) and  $L_z = Q = 0$ .<sup>3</sup>  $\ddot{r}$  in the region around the center where the gravitational force is repulsive is shown in Fig. 11. Intuitively, from these plots one can understand that higher values of  $|a_*|$  produce more energetic and collimated outflows, and that the gas is preferably ejected around the equatorial plane with some open angle that depends on  $|a_*|$ .

## V. DISCUSSION

Let us now discuss the qualitative behavior of the accretion process onto super-spinners that we can expect in a more realistic situation. To this end, we need a few assumptions about the space-time at very small radii and the properties at high temperature of the gas. For example, the naked singularity at  $r = 0$  might be replaced by a very compact object with a finite radius and a surface capable of

<sup>3</sup>In a general Kerr space-time, there is no simple interpretation of  $Q$ . However, in the Schwarzschild case  $a_* = 0$ , the Carter constant reduces to  $L_x^2 + L_y^2$ .



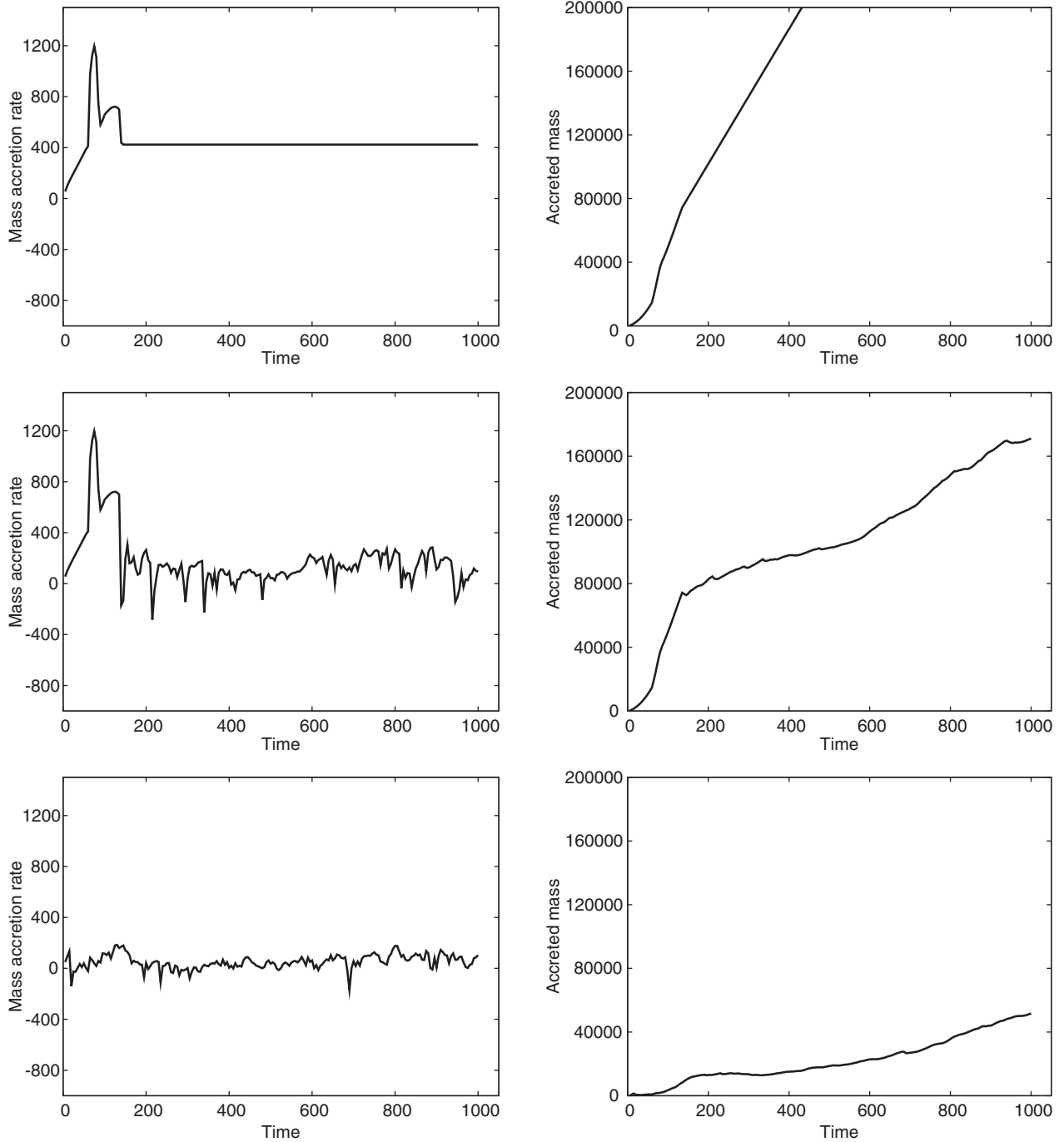


FIG. 9. Mass accretion rate (left panels) and accreted mass (right panels) at  $r = 5M$  for a Kerr super-spinar with  $a_* = 1.1$  (top panels),  $a_* = 1.3$  (central panels), and  $a_* = 3.0$  (bottom panels).

absorbing the accreting matter.<sup>4</sup> Let us also assume that

<sup>4</sup>We warn the reader that this assumption may be an important ingredient in our model. It is likely one of the simplest and most reasonable options (at least in absence of a theory capable of resolving the central singularity), but eventually it is responsible for the quasi-steady-state configuration with strong outflows. If the absorption of gas by the massive object were very suppressed, a quasi-steady-state configuration would be impossible and a cloud would form and grow around the super-spinar.

around the massive body deviations from the Kerr space-time are not significant and that the accreting matter still behaves as a perfect gas. In this case, the gravitational force around the object is everywhere repulsive, except near the equatorial plane [24]. However, as discussed in this paper, in the Bondi-like accretion onto a super-spinar, the gas cannot reach the center from the equatorial plane because of the presence of hot outflows. The result is that the gas approaches the massive object from the poles. At smaller

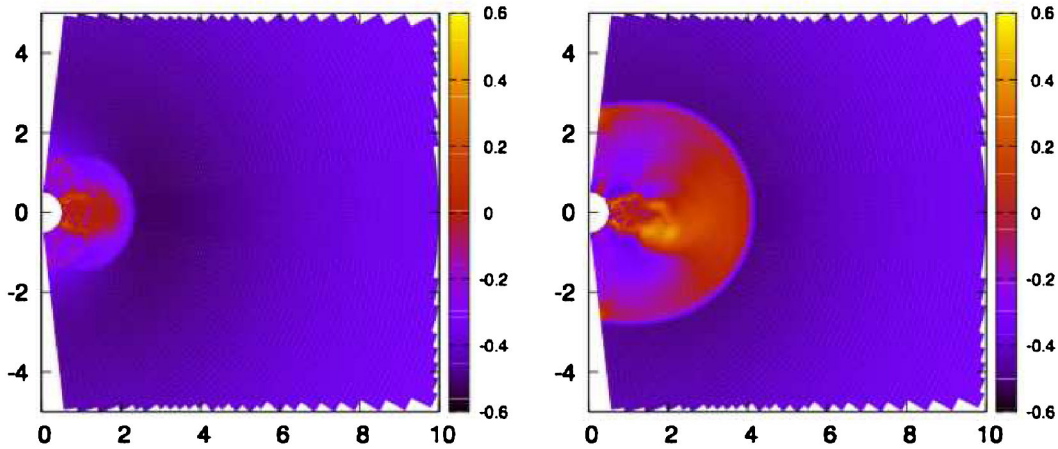


FIG. 10 (color online). Radial velocity of the accreting gas around a super-spiner with  $a_* = 1.1$  (left panel) and  $a_* = 1.2$  (right panel) for  $T_{\max} = 1$  GeV. In the first case, the radius of the convective region is about  $M$ , in the second case about  $3M$ .

and smaller radii, the fluid is more and more compressed, thus reducing further its velocity. Some amount of matter can presumably reach the surface of the super-spiner and be absorbed, but most of the matter probably cannot (especially if the size of the super-spiner is very small). Since the gravitational force is repulsive, the gas cannot pile up indefinitely and some gas is thus ejected to larger radii. Outflows of hot low density gas are produced when some amount of matter is pushed to the region with strongly repulsive gravitational force. Since in the central part of the outflows the gas has a velocity exceeding the escape velocity  $v_{\text{esc}} \sim \sqrt{2M/r}$  (see the left panel of Fig. 1), some material can go to infinity, at least if the finite size of the cloud around the super-spiner is not important in this argument. So, we have energetic outflows, which can escape to infinity and represent a cooling mechanism for the accreting cloud, and low energy outflows, which are ejected to larger radii but are gravitationally bound to the super-spiner. If this is really the case, since the cloud of gas loses energy, eventually the accretion process is not of Bondi type. We may thus recover the accretion discussed in Ref. [24]: the formation of hot outflows stops and the gas can fall to the super-spiner from the equatorial plane, where the gravitational force is attractive (at least for  $|a_*| \geq 1.4$ ; if  $|a_*| < 1.4$  the gas is accumulated around the super-spiner).

In the Bondi phase, super-spinars are presumably much brighter than BHs whose efficiency parameter is about  $10^{-4}$ . Indeed, the gas is not lost behind an event horizon, but orbits in the gravitational potential of the massive object. There might be the possibility that quite exotic matter is produced and ejected to the interstellar medium. Indeed, at very small radii the density and the temperature of the gas can be very high and inelastic scattering between the particles of the gas may produce extremely high-energy, heavy particles. Since blobs of hot gas are continuously ejected to larger radii, super-spinars may enrich the Universe with these products. If the heavy particles are not

highly unstable and can decay into standard model particles in the neighborhood of the super-spiner, the latter might be seen as a source of high-energy cosmic rays.

Last, we are tempted to put forward the possibility that long gamma ray bursts (GRBs) might be explained with the formation of a super-spiner. Of course, one should study the collapse of a star rather than the accretion process onto a super-spiner, but our simulations suggest a few features that look quite promising to produce GRBs. The repulsive gravitational force around super-spinars seems to be able to create collimated jets with high Lorentz factor  $\gamma$ , as shown in Fig. 2. If these jets were able to escape from the collapsing envelope, super-spinars could work as central engines of GRBs. The time variability of the accretion rate found in our simulations might suggest that, for stellar mass super-spinars, even the millisecond time variability observed in GRBs could be reproduced.

## VI. CONCLUSIONS

In this paper, we have investigated the counterpart of the Bondi accretion in the case of super-spinars. Our numerical simulations show that the repulsive gravitational force in the neighborhood of the center can produce powerful outflows of gas, suppressing the accretion process. It is important to notice that the gravitational force becomes repulsive already at radii  $r \sim M$  where, for  $M \gg M_{\text{Pl}}$ , classical GR is presumably reliable. The absence of the horizon can thus lead to the interesting astrophysical implications discussed in this work.

In our simulations, the accretion depends on three parameters: the maximum temperature of the gas,  $T_{\max}$ , the radius of the inner boundary,  $r_{\text{in}}$ , and the dimensionless Kerr parameter,  $a_*$ . We have studied numerically how the variation of  $T_{\max}$ ,  $r_{\text{in}}$ , and  $a_*$  changes our results. Then, we have tried to discuss what can happen in more realistic circumstances that cannot be simulated by the code. Assuming that the super-spiner can be considered as a

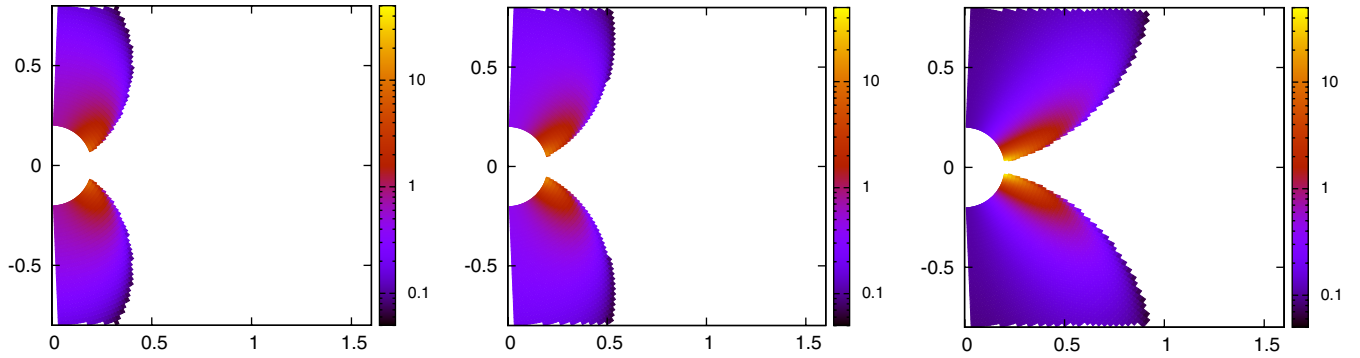


FIG. 11 (color online). Strength of the repulsive gravitational force for a test particle in the region  $r > 0.2M$  around a Kerr super-spinar with  $a_* = 1.1$  (left panel),  $a_* = 1.5$  (central panel), and  $a_* = 3.0$  (right panel). In the white region with  $r > 0.2M$ , the gravitational force is attractive.

compact object with a finite radius and an absorbing surface, and that even in its neighborhood deviations from the classical Kerr metric are not significant, we suggest the following accretion scenario. Only a small fraction of the accreting gas can really reach the surface of the super-spinar and be absorbed, since at smaller and smaller radii the gas velocity decreases, due to two effects: the gravitational force is repulsive and the gas pressure becomes higher and higher. Most of the accreting gas is pushed back to larger radii. Some blobs of hot gas are ejected away with high energy and can escape from the gravitational well of the super-spinar. The rest of the gas is instead cooled and gravitationally bound to the massive object. In this way, the cloud of the accreting gas surrounding the super-spinar cools, less and less gas can enter the region with repulsive gravitational force, and eventually the formation of hot outflows stops. We argue that in this case we recover the accretion process discussed in [24]: the absence of hot outflows let the gas reach the center from the equatorial plane (for  $|a_*| \geq 1.4$ , since in this case the gravitational force is everywhere attractive on the equatorial plane) and then be absorbed by the surface of the super-spinar.

For astrophysical black holes, it is widely believed that jets and outflows are powered by magnetic fields (or maybe even by radiation for high mass accretion rates) and are expected to be ejected from the poles. It is thus likely that the possible observation of powerful equatorial outflows from a black hole candidate is a strong indication that the object is not a black hole, but a super-spinar or, more in

general, a spinning supercompact object with no event horizon. Regions with repulsive gravitational force with features similar to the ones shown in Fig. 11 seem indeed common in space-times describing the gravitational field of spinning masses and containing naked singularities.

At least during the Bondi-like accretion phase, super-spinars should be objects much brighter than usual black holes, because the gas is not quickly lost behind the horizon, but orbits around it. In this phase, there might also be the possibility of producing exotic matter: scattering of the particles near the center, where the density and the temperature can be very high, may produce heavy particles. Another intriguing possibility deserving some attention is that super-spinars might work as the central engine for long GRBs. Indeed, they seem to be able to produce collimated jets with a high Lorentz factor.

## ACKNOWLEDGMENTS

We would like to thank Katherine Freese for collaboration on the early stage of this work. C. B. and N. Y. were supported by World Premier International Research Center Initiative (WPI Initiative), MEXT, Japan. T. H. was partly supported by the Grant-in-Aid for Scientific Research Fund of the Ministry of Education, Culture, Sports, Science and Technology, Japan [Young Scientists (B) 18740144 and 21740190]. R. T. was supported by the Grant-in-Aid for Scientific Research Fund of the Ministry of Education, Culture, Sports, Science and Technology, Japan [Young Scientists (B) 18740144].

- [1] S. W. Hawking and G. F. R. Ellis, *The Large Scale Structure of Space-Time* (Cambridge University Press, Cambridge, U.K., 1973).  
 [2] R. Penrose, Riv. Nuovo Cimento Soc. Ital. Fis. **1**, 257 (1969); *Gen. Relativ. Gravit.* **34**, 1141 (2002).

- [3] B. Carter, *Phys. Rev. Lett.* **26**, 331 (1971).  
 [4] D. C. Robinson, *Phys. Rev. Lett.* **34**, 905 (1975).  
 [5] B. Carter, *Phys. Rev.* **174**, 1559 (1968).  
 [6] S. Chandrasekhar, *The Mathematical Theory of Black Holes* (Clarendon Press, Oxford, U.K., 1983).

- [7] D. Christodoulou, *Commun. Math. Phys.* **93**, 171 (1984).
- [8] A. Ori and T. Piran, *Phys. Rev. D* **42**, 1068 (1990).
- [9] P. S. Joshi and I. H. Dwivedi, *Phys. Rev. D* **47**, 5357 (1993).
- [10] D. Christodoulou, *Ann. Math.* **140**, 607 (1994).
- [11] I. H. Dwivedi and P. S. Joshi, *Commun. Math. Phys.* **166**, 117 (1994).
- [12] S. S. Deshingkar, I. H. Dwivedi, and P. S. Joshi, *Phys. Rev. D* **59**, 044018 (1999).
- [13] T. Harada and K. i. Nakao, *Phys. Rev. D* **70**, 041501 (2004).
- [14] E. G. Gimon and P. Horava, *Phys. Lett. B* **672**, 299 (2009).
- [15] F. de Felice, *Nature (London)* **273**, 429 (1978).
- [16] G. Dotti, R. Gleiser, and J. Pullin, *Phys. Lett. B* **644**, 289 (2007).
- [17] G. Dotti, R. J. Gleiser, I. F. Ranea-Sandoval, and H. Vucetich, *Classical Quantum Gravity* **25**, 245012 (2008).
- [18] V. Cardoso, P. Pani, M. Cadoni, and M. Cavaglia, *Classical Quantum Gravity* **25**, 195010 (2008).
- [19] P. Pani, V. Cardoso, M. Cadoni, and M. Cavaglia, *Proc. Sci. BHsGRandStrings2008* (**2008**) 027.
- [20] C. Bambi and K. Freese, *Phys. Rev. D* **79**, 043002 (2009).
- [21] C. Bambi, K. Freese, and R. Takahashi, [arXiv:0908.3238](https://arxiv.org/abs/0908.3238).
- [22] S. Doeleman *et al.*, *Nature (London)* **455**, 78 (2008).
- [23] R. Takahashi and T. Harada, *Classical Quantum Gravity* **27**, 075003 (2010).
- [24] C. Bambi, K. Freese, T. Harada, R. Takahashi, and N. Yoshida, *Phys. Rev. D* **80**, 104023 (2009).
- [25] C. Bambi, in *Proceedings of the Nineteenth Workshop on General Relativity and Gravitation*, edited by M. Saijo *et al.* (2010), pp. 109–112.
- [26] A. Mignone, G. Bodo, S. Massaglia, T. Matsakos, O. Tesileanu, and C. Zanni, *Astrophys. J. Suppl. Ser.* **170**, 228 (2007).
- [27] <http://plutocode.to.astro.it/index.html>.
- [28] F. Banyuls, J. A. Font, J. M. Ibanez, J. M. Martí, and J. A. Miralles, *Astrophys. J.* **476**, 221 (1997).
- [29] E. P. Liang, *Phys. Rep.* **302**, 67 (1998).
- [30] F. C. Michel, *Astrophys. Space Sci.* **15**, 153 (1972).
- [31] S. L. Shapiro and S. A. Teukolsky, *Black Holes, White Dwarfs, and Neutron Stars: The Physics of Compact Objects* (Wiley, New York, New York, 1983).